

Technical Reference Publication

S083A(NC)



Document provided courtesy of

SpaceAge Control, Inc.

An ISO 9001/AS9000-Compliant Company
38850 20th Street East • Palmdale, CA 93550 USA
+1-661-273-3000
email@spaceagecontrol.com
<http://spaceagecontrol.com/>

Engine Sensors
Environmental Control System (ECS) Sensors
Non-Aerospace Air Data Products
Multi-Axis Displacement Sensors
Position Transducers

NACA TN 4351 56901

NATIONAL ADVISORY COMMITTEE FOR AERONAUTICS



TECHNICAL NOTE 4351

SUMMARY OF METHODS OF MEASURING
ANGLE OF ATTACK ON AIRCRAFT

By William Gracey

Langley Aeronautical Laboratory
Langley Field, Va.



Washington
August 1958

AFMDC
TECHNICAL LIBRARY
AEL 2311



NATIONAL ADVISORY COMMITTEE FOR AERONAUTICS

TECHNICAL NOTE 4351

SUMMARY OF METHODS OF MEASURING

ANGLE OF ATTACK ON AIRCRAFT

By William Gracey

SUMMARY

Wind-tunnel calibrations of three types of angle-of-attack sensing devices - the pivoted vane, the differential pressure tube, and the null-seeking pressure tube - are presented. The pivoted vane has been used primarily in the flight testing of airplanes and missiles, whereas the null-seeking pressure tube has been used almost exclusively in the service operation of airplanes. The differential pressure tube has not been used to any great extent as a flight instrument.

Flight data on the position errors for three sensor locations - ahead of the fuselage nose, ahead of the wing tip, and on the forebody of the fuselage - are also presented. For operation throughout the subsonic, transonic, and supersonic speed ranges, a position ahead of the fuselage nose will provide the best installation. If the shape of the fuselage nose is not too blunt, the position error will be essentially zero when the sensor is located 1.5 or more fuselage diameters ahead of the fuselage.

Various methods for calibrating angle-of-attack installations in flight are briefly described.

INTRODUCTION

Angle of attack is defined as the angle between the relative wind in the plane of symmetry and the longitudinal axis of the airplane. The measurement of this quantity has received increasing attention in recent years because of its requirement for fire control, cruise control, and stall warning.

Sensing devices for measuring angle of attack may be located either ahead of the aircraft (usually on booms mounted on the wing tip or the

fuselage nose) or on some part of the aircraft itself. For any position on or near the aircraft, however, the sensing device will measure the local rather than the true angle of attack. The amount by which the local angle of attack differs from the true angle of attack is called the position error of the installation. This error varies with the lift coefficient and Mach number of the aircraft. For some locations of the sensing device, the position error may also vary with changes in the configuration of the aircraft, for example, flap deflection, landing-gear extension, and so forth.

The overall error of an installation includes errors peculiar to the sensing device in addition to the errors due to the location of the device. The errors of the sensing device are generally determined by wind-tunnel tests. The position error, on the other hand, must be determined by calibration of the installation in flight. In accelerated maneuvers, additional errors may be introduced by such items as the pitching velocity of the aircraft, boom bending, fuselage flexibility, and lag in the transmission system of the angle-of-attack instrumentation.

A description of various types of angle-of-attack devices and their application to stall warning is presented in reference 1. A comprehensive survey of possible types of instrumentation for the measurement of angle of attack on aircraft is given in reference 2. In a similar study (ref. 3) a method is developed for determining angles of attack and sideslip from measurements of the motions of the aircraft.

The present report summarizes experimental data on sensing devices which have found practical application in the testing of airplanes and missiles or which have been test evaluated for possible use on aircraft. The position errors of several types of installation and some flight calibration methods for determining these errors are also presented.

SYMBOLS

α	angle of attack (angle between relative wind in the plane of symmetry and the longitudinal axis of the airplane), deg
α_1	local angle of attack, deg
$\Delta\alpha$	angle-of-attack error ($\alpha_1 - \alpha$), deg
β	angle of sideslip, deg
Δp	pressure difference between orifices on differential pressure tube

q	dynamic pressure
M	Mach number
C_N	normal-force coefficient
c	local wing chord
D	maximum effective fuselage diameter
x	distance of sensor ahead of wing or fuselage
l	cone length (conical differential pressure tube)

SENSING DEVICES

The types of sensing devices which have been used for the measurement of angle of attack are the pivoted vane, the differential-pressure tube, and the null-seeking pressure tube. The pivoted vane has been used primarily in the flight testing of airplanes and missiles, whereas the null-seeking pressure tube has been used almost exclusively in the service operation of airplanes. The differential pressure tube has not been used to any great extent as a flight instrument.

Pivoted Vanes

A pivoted vane is a mass-balanced wind vane free to align itself with the direction of the air flow. The vane may be mounted either ahead of a boom support or on a transverse shaft which is attached to a boom or to the body of the airplane. The angles measured by a vane mounted on a boom will be influenced by (1) distortion of the flow when the boom is inclined to the flow (upwash effect), (2) asymmetry of the vane due to imperfections in manufacture (floating angle), and (3) bending of the boom support due to air loads.

In maneuvering flight, additional errors may be introduced because of further bending of the boom (as a result of normal and pitching accelerations) and the pitching velocity of the airplane. In the case of a flexible airplane, consideration may also have to be given to the effects of flexibility of the structure.

The magnitude of the upwash effect of both axially and transverse-mounted vanes depends on the diameter of the boom support. For a vane on a transverse shaft, the magnitude of the effect also depends upon the

distance of the vane from the axis of the boom. In this case the effect of upwash may be minimized by locating the vane at least two boom diameters from the boom axis (ref. 4).

Corrections for upwash around the boom may be determined by calibrating the sensing device in a wind tunnel. The floating angle of the vane can be determined at the same time by calibrating the device in upright and inverted positions. The floating angle is determined as one-half the difference between indications in the two positions. As noted in reference 4, the floating angle may also be determined in flight by calibrating the vane in upright and inverted positions on successive flights. In this method a second angle-of-attack system is required as a reference for the vane measurements.

As noted previously, bending of the boom may occur as a result of aircraft air loads and aircraft acceleration. Deflection of the boom due to air loads may be estimated from information on drag coefficients of cylinders or may be computed from wind-tunnel measurements of the particular boom being used. Boom deflections due to normal and pitching accelerations may be computed from the recorded values of the aircraft accelerations and from ground calibrations of the boom deflection as obtained by applying various weights to the boom. A more direct measure of the deflection due to both air loads and accelerations is one in which the boom is photographed in flight with a camera installed in the fuselage of the airplane. A detailed discussion of the methods of determining upwash effect, floating angle, and boom bending is given in reference 4.

Axially mounted pivoted vanes.- A pivoted vane designed for mounting ahead of a boom support is described in reference 5. As shown by the diagram on figure 1(a), the sensor consists of a conical body with a triangular vane attached to the rear portion of the cone. This sensor was developed for the testing of missiles and is, for this reason, comparatively small. The length of the conical body is $3\frac{1}{4}$ inches and the span of the vane about $2\frac{3}{4}$ inches. The shaft to which the vane is connected is designed for attachment to a $\frac{3}{4}$ -inch-diameter boom.

The vane unit has a maximum range of $\pm 15^\circ$. The results of wind-tunnel tests (ref. 5) for an angle-of-attack range of -4° to 12° ($\beta = 0^\circ$) are presented in figure 1(b). The data were obtained at Mach numbers of 0.85, 0.95, and 1.20. The large scatter of the test points at $M = 0.85$ and 0.95 is believed to be due to friction or play in the transmitting linkage and sliding-core pickup.

Transverse-mounted pivoted vanes.- A type of pivoted vane in which the vane is mounted on a shaft attached to the side of the boom support

is shown in figure 2(a). The sensing device shown in this figure incorporates two vanes oriented 90° apart. In addition to measurements of angles of attack and sideslip, this instrument also measures pitot and static pressures. This sensing device was especially developed for the flight testing of research aircraft and is designed for mounting on a fuselage-nose boom.

The results of a wind-tunnel calibration (ref. 6) of the angle-of-attack vane at $M = 0.6$ to 1.10 are presented in figure 2(b). The vane was calibrated over an angular range of -5° to 25° . The slopes of the curves are a measure of the upwash around the boom. The errors at $\alpha = 0$ would appear to be an indication of the floating angle of the vane.

Wind-tunnel tests of another instrument of this type at higher Mach numbers (1.61 to 2.01) are reported in reference 7. The results of these tests which covered an angle-of-attack range of -3° to 20° at $M = 1.61$ and -3° to 24° at $M = 2.01$ are presented in figure 2(c). In these tests, three vanes were tested to check any variations due to manufacturer. The results showed no significant differences in the floating angles of the three vanes.

Differential-Pressure Tube

An angle-of-attack sensor of the differential-pressure-tube type consists of two orifices oriented at equal angles on either side of the longitudinal axis of the tube. The pressure difference which exists at the two orifices when the tube is inclined to the flow is a measure of the angle of attack of the tube. At any given angle of attack the magnitude of this pressure difference depends principally on the shape of the nose of the tube, on the angular position of the orifices, and to some extent on Mach number and Reynolds number.

The two types of nose shape which have been used to the greatest extent in the design of differential-pressure sensors are the hemisphere and the cone. For these shapes the greatest sensitivity of the tube to angle of attack can be achieved by orientating the orifices about 90° apart on the hemisphere (see data in ref. 8) or, in the case of the cone, by using a 90° cone angle.

As the angle of attack of a differential pressure sensor is a function of the ratio of the pressure difference to the impact pressure, the use of this type of tube requires the measurement of two quantities. If recording instruments are used, the two quantities can be recorded separately and the angle of attack determined by computation. If, however,

a direct indication of the angle of attack is desired, a pressure-ratio type of instrument must be employed.

Data from wind-tunnel tests of differential-pressure sensors having hemispherical nose shapes are presented in figures 3 and 4. The sensor shown in figure 3(a) was about $1\frac{1}{4}$ inches in diameter with two orifices spaced 90° apart. The data for this sensor were from a report of limited availability by G. F. Moss and N. K. Walker of the British Royal Aircraft Establishment. The tests were conducted at a Mach number of about 0.11 through an angle-of-attack range of $\pm 20^\circ$. The variation of $\Delta p/q$ with α for these test conditions is given in figure 3(b). The two sensors shown in figure 4(a) were $1/2$ inch in diameter and were tested by the Engineering Physics Department at Cornell Aeronautical Laboratory, Inc. The orifices of one of the tubes were spaced 60° apart and those of the other, 90° apart. The tests covered a range of Mach number of 0.3 to 0.8 and an angular range of 0° to 20° . Sample results of the tests at $M = 0.35$ and 0.60 are presented in figure 4(b). These data show that the tube with the orifices spaced 90° apart is more sensitive to angle of attack than the tube with orifices spaced 60° apart. The data also show the sensitivity of both tubes to decrease as the Mach number increases. A comparison of the data in figures 3 and 4 shows the sensitivity of tube A in figure 4 to be greater than that of the tube shown in figure 3 despite the fact that the orifices on both of the tubes are spaced 90° apart. The Mach number trend shown in figure 4 does not account for this difference and no other explanation for the difference can be found in the reports of these two tests.

The use of conical nose shapes for measurements at supersonic speeds has received considerable attention because the measurement of total pressure at the nose of the cone, in combination with the pressures on the surface of the cone, can provide indications of Mach number and static pressure as well as angles of attack and sideslip. Wind-tunnel tests to determine the accuracy with which Mach number and angle of attack can be calculated from the pressures on a 15° cone at $M = 1.59$ are reported in reference 9.

Wind-tunnel data of conical-nosed tubes having apex angles of 30° , 40° , and 50° were also made at the Cornell Aeronautical Laboratory, Inc. The body diameter of each tube was $1/2$ inch and the orifices on each of the tubes were located $2/3$ of the cone length behind the apex. (See fig. 5(a).) The tests were conducted at $M = 0.30$ to 0.65 through an angle-of-attack range of 0° to 20° . Sample calibrations of the tubes at $M = 0.35$ and 0.60 are presented in figure 5(b). These curves show the sensitivity of the tubes to decrease as the apex angle decreases. For the range of Mach numbers covered by the tests, the effect of Mach number on the sensitivity is small for the 50° probe and negligible for the 30° and 40° probes.

Calibrations at transonic speeds of a conical-nosed sensor having an apex angle of 45° were performed by the wing-flow method. (See ref. 10.) The tube was 1 inch in diameter and the orifices were located 0.674 inch from the nose. (See fig. 6(a).) The tests were conducted at $M = 0.70$ to 1.10 through an angular range of -10° to 50° . A single curve, representing the mean of the test data obtained throughout the test range is presented in figure 6(b). Although the scatter of the test points as presented in reference 10 was as much as 1.5° at some angles of attack, there was no consistent variation of $\Delta p/q$ with Mach number. This scatter of the test data and the fact that the curve does not pass through the origin was noted in reference 10 as being the result of play in the actuating mechanism used to rotate the tube through the angle-of-attack range.

Supersonic wind-tunnel tests of a conical-nosed sensor having a 20° apex angle are reported in reference 11. The body of the sensor was $3/8$ inch in diameter with orifices located $1/4$ inch from the apex. (See fig. 7(a).) The tests were conducted at $M = 1.5, 1.6,$ and 1.7 through a range of angle of attack of -5° to 10° . The results of the tests are presented in figure 7(b). No explanation is given in reference 11 for the fact that the curves for $M = 1.5$ and 1.6 do not pass through the origin.

Null-Seeking Pressure Sensor

A null-seeking pressure sensor for measuring angle of attack consists of (1) a rotatable tube with two orifices disposed at equal angles to the axis of the tube, (2) a pressure-sensitive device for detecting the pressure difference between the two orifices when the tube is inclined to the flow, (3) a mechanism for rotating the tube to the null-pressure position, and (4) instrumentation for measuring the angular position of the tube. The advantages of this tube as compared with the differential-pressure tube are (1) the measurements are independent of impact pressure, Mach number, and Reynolds number and (2) the differential-pressure sensing elements can be comparatively sensitive because the operating differential pressures should be always near zero, provided of course, the response of the system is sufficiently rapid.

An example of a sensing device of the null-seeking pressure-tube type is illustrated in figure 8(a). This device consists of a rotatable cylindrical tube which protrudes through the wall of the fuselage and an air chamber system which is housed inside the fuselage. The tube is $3/8$ inch in diameter and about $3\frac{3}{8}$ inches long and incorporates a pair of slots spaced 60° apart. The interior of the tube is divided into two sections which vent to a pair of air chambers formed by a swivel paddle

vane. A pressure difference at the two slots causes rotation of the paddle vane which, by means of a linkage, rotates the pressure tube until the pressures are equalized. The angular position of the probe is then measured by a potentiometer.

Wind-tunnel tests of this device at 75 to 125 miles per hour are reported in reference 12. The instrument was calibrated over an angular range of -15° to 14° . Sample results of the tests are presented in figure 8(b) for a speed of 75 miles per hour ($M = 0.10$). As shown by this figure the mean error was within $\pm 0.1^{\circ}$ over the angular range of the tests. The scatter of the test points about the mean curve was within about $\pm 0.2^{\circ}$. Dynamic-response tests indicated that at frequencies between 0.8 and 1.8 cps the amplitude frequency response was about 90 percent at 100 miles per hour and 97 percent at 150 miles per hour.

Another type of null-seeking pressure tube (fig. 9(a)), designed for mounting on the end of a horizontal boom, is described in reference 8. The sensing element of this device consists of an ellipsoidal nose tube, 2 inches in diameter, with two orifices oriented at equal angles with respect to the longitudinal axis of the tube. The orifices are connected to a sensitive pressure capsule located in the nose of the tube. Deflection of the capsule produces a signal which operates a servomechanism which, in turn, rotates the tube to the null-pressure position. The position of the tube is then measured by a synchro-system.

The results of low-speed wind-tunnel tests of this device are presented in figure 9(b). The error, which is caused by the upwash around the boom, varies from -1° at an angle of attack of -10° to 1.2° at an angle of attack of 12° . The accuracy of the measurements is $\pm 0.1^{\circ}$. Dynamic-response tests indicated that, with the type of servomechanism used with this tube, the amplitude frequency response is close to 100 percent up to 1.3 cycles per second.

POSITION ERRORS

Because of the flow field created by the aircraft, the flow angle at any given location in the vicinity of the aircraft will generally differ from the true angle of attack of the aircraft. At subsonic speeds the effects of the flow field extend in all directions from the aircraft. At supersonic speeds the effects are confined to regions behind the shock waves which form ahead of the aircraft. Thus, angle-of-attack sensors located ahead of the foremost airplane shock should be unaffected by the flow field of the aircraft at supersonic speeds.

As the flow field around each aircraft configuration is unique, the position error (that is, the difference between local and true angles of attack) at a given location with respect to the aircraft will vary from one aircraft to another. Exact values of the position errors of a given installation on a specific aircraft, therefore, can be determined only by calibration of the installation in flight. Flight calibrations of installations on specific airplanes, however, can provide an indication of relative magnitudes and trends of the position errors for given locations of the sensing device. Three sensor positions which have proved successful and which have been used to the greatest extent are positions ahead of the fuselage nose, ahead of the wing tip, and on the forebody of the fuselage.

Positions Ahead of Fuselage Nose

At speeds below the Mach number at which the fuselage bow shock passes the angle-of-attack sensor, the position error at a given distance ahead of the fuselage depends on the maximum diameter of the fuselage and the shape of the fuselage nose section.

The variation of local angle of attack with distance ahead of a fuselage having a rounded ogival nose shape is presented in figure 10 for a constant Mach number of 0.80 (unpublished data obtained at the Ames Aeronautical Laboratory). The data in this figure show that for each value of normal-force coefficient the local angle of attack decreases (and approaches the true angle of attack) as the distance from the nose increases.

The variation of local angle of attack with distance ahead of the nose of a fuselage having a nose inlet is presented in figure 11 for a constant Mach number of 0.81. (See ref. 13.) The flow-angle variation of this installation is similar to that for positions ahead of the fuselage having a rounded ogival nose shape. The data from the two airplanes indicate that, for fuselage nose shapes no blunter than these, the local angle of attack will be very nearly the true angle of attack at positions 1.5 or more fuselage diameters ahead of the fuselage nose. Because an angle-of-attack sensor located ahead of the nose will come under the influence of only one shock (the fuselage bow wave), sensor locations ahead of the fuselage nose are considered to be preferable to wing tip and fuselage surface positions, particularly for transonic and supersonic operation.

Positions Ahead of Wing Tip

Prior to the passage of the wing and fuselage bow shocks over the sensor, the position error at a given distance ahead of the wing of an

airplane is determined by the maximum thickness of the local airfoil, the shape of the airfoil section, the sweepback angle of the wing, and the spanwise location. At the Mach numbers at which the wing and fuselage bow shocks pass or are in the vicinity of the sensor, large errors may be introduced due to variations of angle of sideslip.

At subsonic speeds the position error varies with distance ahead of the wing in a manner similar to that for positions ahead of the fuselage nose. Because of the lifting characteristic of the wing, however, the position errors of wing-tip installations are apt to be larger than those of comparable fuselage-nose installations. A calibration of a differential-pressure type angle-of-attack sensor located 0.5 chord length ahead of the wing tip of an airplane is presented in figure 12 (data from Cornell Aero. Lab., Inc., for $M = 0.3$).

Positions on the Surface of the Fuselage Nose

Calibrations of an angle-of-attack sensor on the surface of the fuselage nose of an airplane were determined from tests reported in reference 13. The sensor was a null-seeking pressure type and was located near the center line of the fuselage and about midway from the nose to the leading edge of the wing. The local angle of attack indicated by the sensor was compared with the angle of attack measured by a vane-type sensor located about $1\frac{2}{5}$ fuselage diameters ahead of the fuselage nose. The measurements from the vane were considered to represent the true angles of attack of the airplane.

The tests were conducted over a Mach number range of 0.6 to 1.02. Sample calibrations of the installation at $M = 0.6, 0.81, \text{ and } 0.92$ are given in figure 13. These data, as well as those at the other test speeds, show a linear variation of local angle of attack with true angle of attack. The data also show that for constant angle of attack the local angle of attack decreases as the Mach number increases. In addition, the local angle of attack is shown to change about 1.6° for each degree change in true angle of attack. For other locations of the sensor on the nose and for other fuselage nose shapes, the variations of local angle of attack with true angle of attack will, of course, be different.

The effect of angle of sideslip on the angle of attack indicated by the sensor was determined at constant true angles of attack at $M = 0.70 \text{ to } 0.91$. As shown by the curves in figure 14, the variation of indicated angle of attack with sideslip was linear and amounted to 0.1° angle of attack for each degree of sideslip. These data also indicate that for small sideslip angles the effect of sideslip can be eliminated by installing sensors on each side of the fuselage and averaging the two indications.

FLIGHT CALIBRATION METHODS

An angle-of-attack installation may be calibrated in flight by any one of a number of methods. Some of the methods are applicable only to unaccelerated flight, whereas others may be employed for maneuvering flight as well. As the instrumentation and procedure for some of the methods are very involved, only a general description of the methods will be given here.

Attitude-Angle Method

In level unaccelerated flight and in the absence of vertical air currents, the attitude angle of an airplane is equal to its angle of attack. In localities where the horizon is not obscured by haze, the attitude angle can be measured easily by photographing the horizon from a camera installed in the airplane and directed either forward or to the side. For a camera directed forward, corrections must be applied for the curvature of the earth. (See ref. 14.)

In those cases where it is impractical to photograph the horizon, the attitude angle of the airplane may be determined by photographing the sun. The elevation angle of the sun is determined from the longitude and latitude of the airplane, from navigation tables, and from a precise measure of time. (See ref. 15.)

The attitude angle of the aircraft may also be measured with a pendulum inclinometer. (See ref. 16.) The angles measured by this instrument, however, are subject to errors due to variations in longitudinal acceleration. For this reason, the use of an inclinometer will generally prove more unsatisfactory than the use of horizon or sun cameras, both of which are unaffected by aircraft acceleration.

The greatest difficulty in applying the attitude-angle method is encountered in attempting to maintain level flight. Standard aircraft altimeters are not sufficiently sensitive to provide the high order of accuracy usually required. For this reason, a sensitive recording statoscope should be used for detecting deviations from constant altitude. If appreciable changes in altitude occur during the tests, the attitude-flight-path-angle method described in the next section should be applied.

Another difficulty in the application of the attitude angle method involves the effect of vertical air currents. Best results would appear to be obtained by conducting the tests at low altitudes (preferably over

a large body of water) because the magnitude of the vertical air currents would be expected to be smaller than at higher altitudes.

Attitude—Flight-Path Angle Method

A method by which an installation can be calibrated when the airplane is changing altitude involves the measurement of flight-path angle in conjunction with the attitude angle. The flight-path angle is determined from simultaneous measurements of the vertical velocity and the velocity along the flight path.

The vertical velocity may be measured with a recording statoscope or by integrating a time history of the vertical acceleration, which may be calculated from the recorded normal and longitudinal accelerations and the attitude angle.

As discussed in the previous section, the attitude angle may be measured with a horizon camera or a sun camera. In some cases it may be more convenient to measure only the initial attitude angle with a sun camera, horizon camera, or inclinometer and then to determine the change in attitude angle from measurements with an attitude gyroscope or from integration of the recorded pitching velocity.

The calculation of angle of attack by the attitude—flight-path angle method requires that the records of each of the measured quantities have a time scale and a means of synchronization.

Fuselage-Nose-Boom Method

In the fuselage-nose-boom method the local angle of attack at a point a considerable distance ahead of the fuselage is considered to represent a close approximation to the true angle of attack of the airplane. The angle-of-attack measurement is most conveniently made by means of a pivoted vane installed on a boom extending ahead of the fuselage nose. Tests to determine the variation of local angle of attack with distance ahead of the fuselages of an airplane (ref. 13) showed that, with increasing distance ahead of the fuselage, the local angle of attack approached the true angle of attack asymptotically and that at a distance of at least 1.5 fuselage diameters the local angle of attack was essentially equal to the true angle of attack. Calibrations in which this method was employed in tests on another airplane are reported in reference 17. When the tests are conducted in accelerated flight, corrections must, of course, be applied for bending of the boom, pitching velocity of the airplane, and bending of the fuselage.

Ground Photographic Methods

A method has been developed in which the angle of attack is determined from the flight-path angle as determined from a camera on the ground and the attitude angle as measured by a camera installed in the airplane. The direction and velocity of the wind are determined from photographs by the ground camera of smoke puffs released from the airplane. The method was developed for the special case of an airplane diving toward a ground target at a predetermined dive angle. As described in references 18 and 19, the method requires that the ground camera be located at the center of the target and elevated to the proposed dive angle of the airplane. The camera in the airplane photographs the ground target during the dive. An extension of this method to permit calibration during the pull-up following the dive required the use of two ground cameras and three surveyed ground markers. (See ref. 20.)

CONCLUDING REMARKS

Wind-tunnel calibrations of three types of angle-of-attack sensing devices - the pivoted vane, the differential pressure tube, and the null-seeking pressure tube - have been presented. The pivoted vane has been used primarily in the flight testing of airplanes and missiles, whereas the null-seeking pressure tube has been used almost exclusively in the service operation of airplanes. The differential pressure tube has not been used to any great extent as a flight instrument.

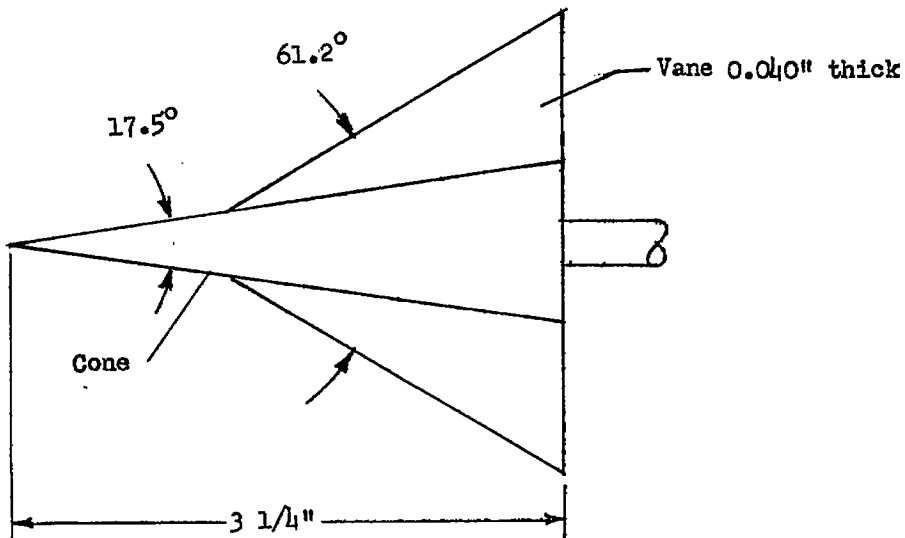
Flight data on the position errors of three sensor locations - ahead of the fuselage nose, ahead of the wing tip, and on the forebody of the fuselage - have also been presented. For operation throughout the subsonic, transonic, and supersonic speed ranges, a position ahead of the fuselage nose will provide the best installation. If the shape of the fuselage nose is not too blunt, the position error will be essentially zero when the sensor is located 1.5 or more fuselage diameters ahead of the fuselage.

Langley Aeronautical Laboratory,
National Advisory Committee for Aeronautics,
Langley Field, Va., March 24, 1958.

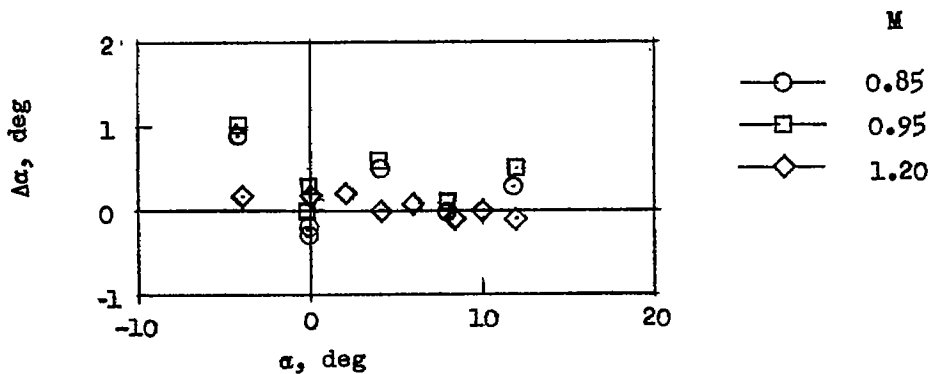
REFERENCES

1. Zalovcik, John A.: Summary of Stall-Warning Devices. NACA TN 2676, 1952.
2. Emerson, F. M., Gardner, F. H., Gruenwald, G. D., Olshausen, R., and Sloma, L. V.: Study of Systems for True Angle of Attack Measurement. WADC Tech. Rep. 54-267, U. S. Air Force, May 1955.
3. Smetana, Frederick O., and Stuart, Jay Wm., Jr.: A Study of Angle-of-Attack Angle-of-Sideslip Pitot-Static Probes. WADC Tech. Rep. 57-234, AD 118209, U. S. Air Force, Jan. 1957.
4. McFadden, Norman M., Holden, George R., and Ratcliff, Jack W.: Instrumentation and Calibration Technique for Flight Calibration of Angle-of-Attack Systems on Aircraft. NACA RM A52I23, 1952.
5. Mitchell, Jesse L., and Peck, Robert F.: An NACA Vane-Type Angle-of-Attack Indicator for Use at Subsonic and Supersonic Speeds. NACA TN 3441, 1955. (Supersedes NACA RM L9F28a.)
6. Pearson, Albin O., and Brown, Harold A.: Calibration of a Combined Pitot-Static Tube and Vane-Type Flow Angularity Indicator at Transonic Speeds and at Large Angles of Attack or Yaw. NACA RM L52F24, 1952.
7. Sinclair, Archibald R., and Mace, William D.: Wind-Tunnel Calibration of a Combined Pitot-Static Tube and Vane-Type Flow-Angularity Indicator at Mach Numbers of 1.61 and 2.01. NACA TN 3808, 1956.
8. Young, D. W.: Development of the Null Pressure Type Angle of Attack and Angle of Yaw Indicator. AF Tech. Rep. 6280, ASTIA Doc. Nr. AD 118025, Wright Air Dev. Center, U. S. Air Force, Jan. 1957.
9. Cooper, Morton, and Webster, Robert A.: The Use of an Uncalibrated Cone for Determination of Flow Angles and Mach Numbers at Supersonic Speeds. NACA TN 2190, 1951.
10. McClanahan, Herbert C., Jr.: Wing-Flow Investigation of a 45° Cone as an Angle-of-Attack Measuring Device at Transonic Speeds. NACA RM L51E16, 1951.
11. Davis, Theodore: Development and Calibration of Two Conical Yawmeters. Meteor Rep. UAC-43, United Aircraft Corp., Oct. 1949.

12. Aircraft Laboratory Aeronautics Division: Specialties Angle of Attack Indicator. Memo. Rep. WCNSW 655-1605-1, Wright Air Development Center, U. S. Air Force, Mar. 5, 1952.
13. McFadden, Norman M., Rathert, George A., Jr., and Bray, Richard S.: Flight Calibration of Angle-of-Attack and Sideslip Detectors on the Fuselage of a 35° Swept-Wing Fighter Airplane. NACA RM A52A04, 1952.
14. Seeley, L. W.: A Simple Technique for the Measurement of Aircraft Angle of Attack. NAVORD Rep. 1294 (NOTS 364), U. S. Naval Ordnance Test Station, Inyokern (China Lake, Calif.), Mar. 8, 1951.
15. Zalovcik, John A., Lina, Lindsay J., and Trant, James P., Jr.: A Method of Calibrating Airspeed Installations on Airplanes at Transonic and Supersonic Speeds by the Use of Accelerometer and Attitude-Angle Measurements. NACA Rep. 1145, 1953. (Supersedes NACA TN 2099 by Zalovcik and NACA TN 2570 by Lina and Trant.)
16. Seeley, Leonard W.: Flight Investigation of a 1-g Angle-of-Attack Position-Error Calibration Technique. NAVORD Rep. 2025 (NOTS 681), U. S. Naval Ord. Test Station, Inyokern (China Lake, Calif.), Apr. 17, 1953.
17. Seeley, Leonard W.: Flight Investigation of the Position Error Associated With Local Air Flow Detectors Installed on a Model F9F-2 Aircraft. NAVORD Rep. 2014 (NOTS 646), U. S. Naval Ord. Test Station, Inyokern (China Lake, Calif.), Mar. 2, 1953.
18. Hibbs, William H., Allen, Robert B., and Ward, Mary C.: Development of a Target-Center Camera and Its Applications in Fire-Control Research. NAVORD Rep. 1026 (NOTS 145), U. S. Naval Ordnance Test Station (Inyokern, Calif.), Sept. 3, 1948.
19. Keuper, R. F.: Aircraft Angle-of-Attack Determination by Ground Photography. NAVORD Rep. 1037 (NOTS 156), U. S. Naval Ord. Test Station (Inyokern, Calif.), Sept. 26, 1948.
20. Strand, Otto Neall: A General Method for the Photographic Determination of Aircraft Attitude, Angle of Attack, and Related Parameters. NAVORD Rep. 3506 (NOTS 1135), U. S. Naval Ord. Test Station (China Lake, Calif.), May 26, 1955. (Available from ASTIA as AD No. 81135.)

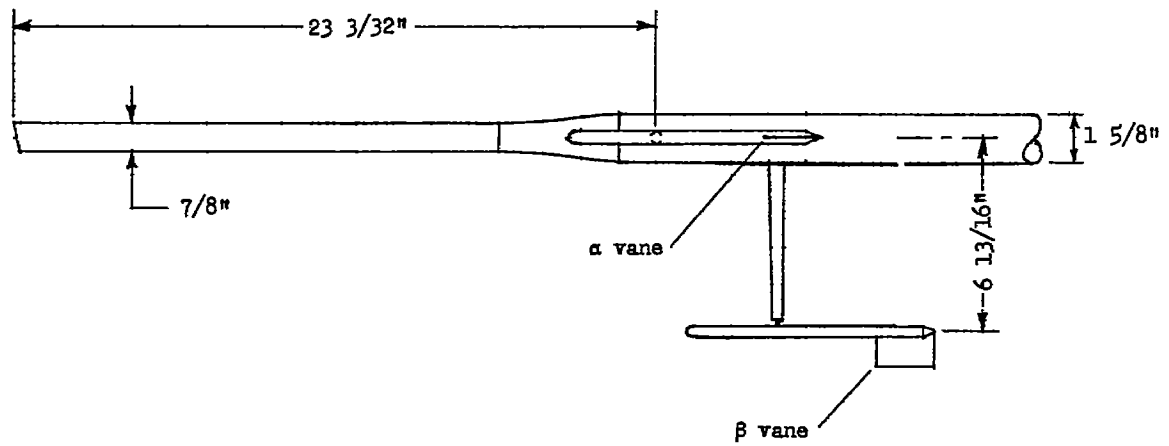


(a) Sensor.

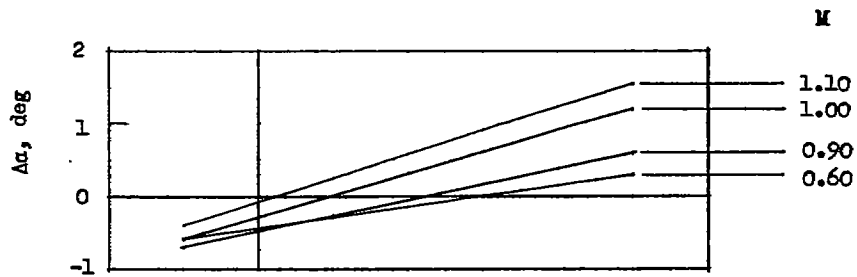


(b) Calibration.

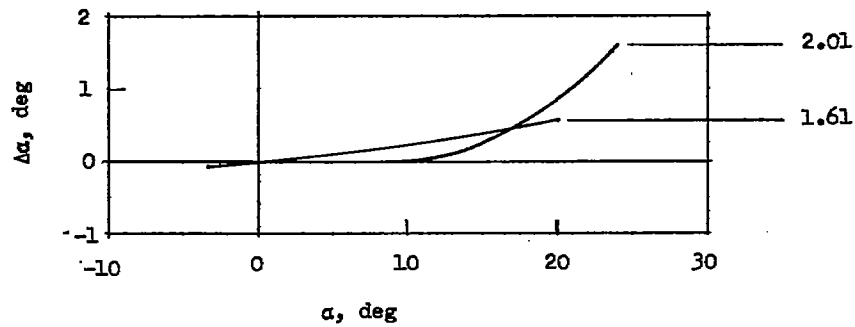
Figure 1.- Calibration of axially mounted pivoted vane at transonic speeds (ref. 5). $\beta = 0^\circ$.



(a) Sensor.

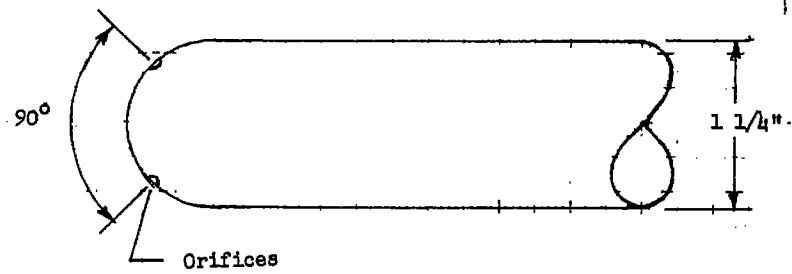


(b) Calibration; transonic (ref. 6).

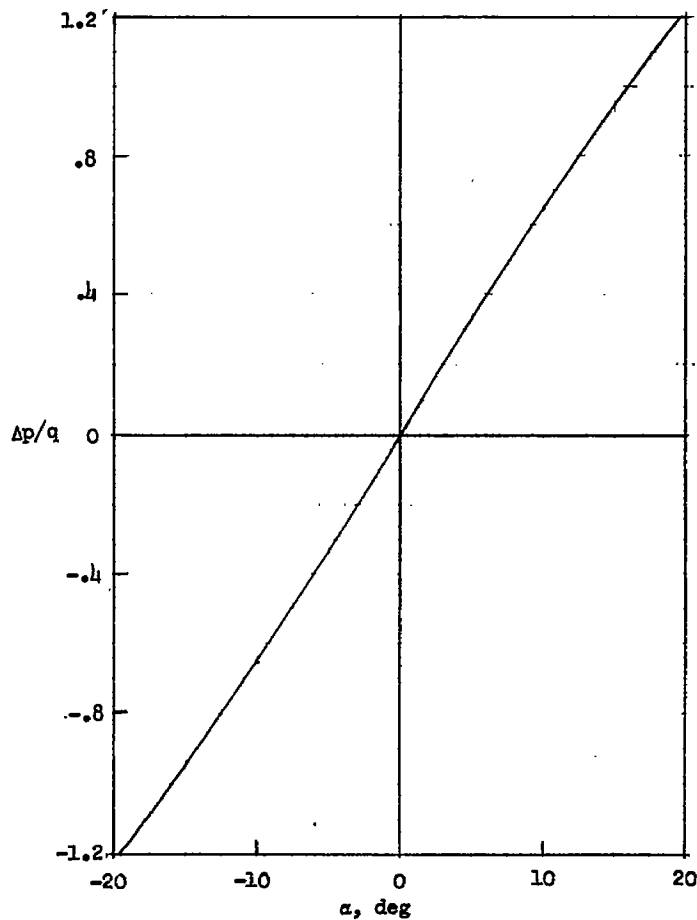


(c) Calibration; supersonic (ref. 7).

Figure 2.- Calibration of transverse-mounted pivoted vane at transonic and supersonic speeds (refs. 6 and 7). $\beta = 0^\circ$.

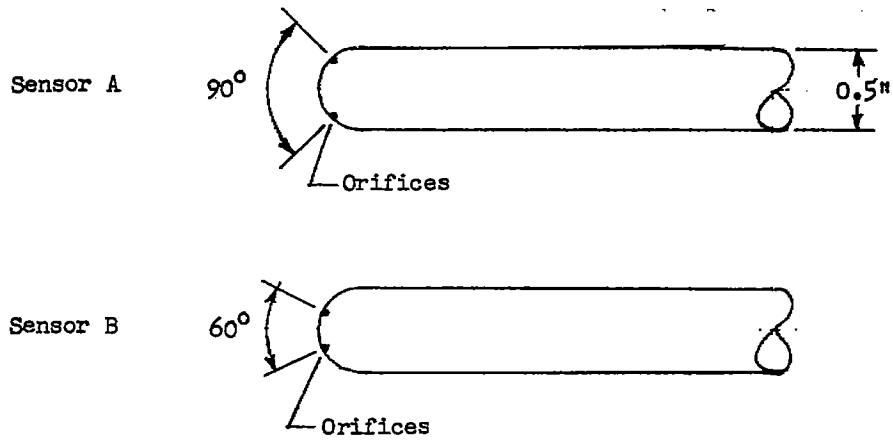


(a) Sensor.

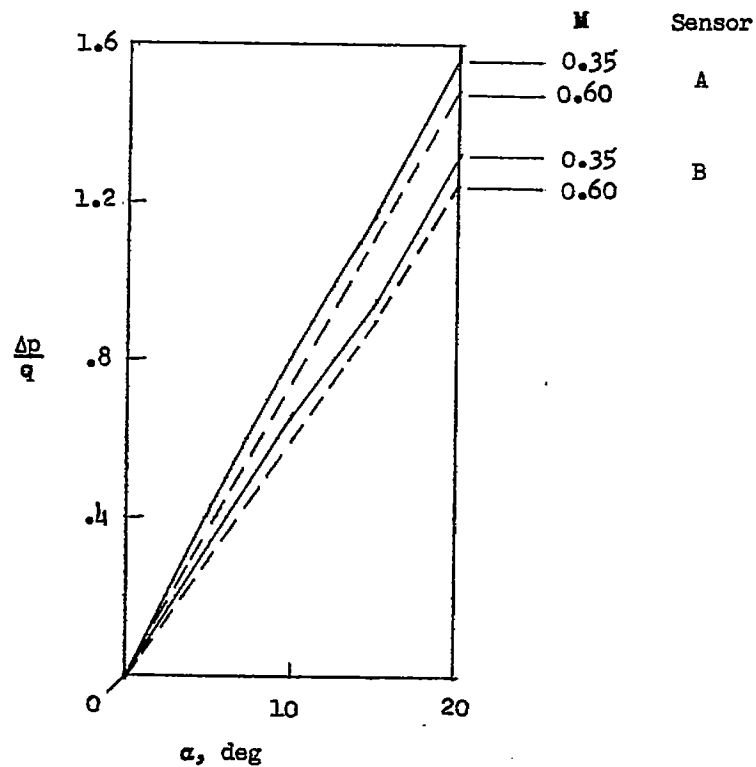


(b) Calibration.

Figure 3.- Variation of $\Delta p/q$ with α of a differential pressure sensor having a hemispherical nose shape from unpublished British tests. $M = 0.11$; $\beta = 0^\circ$.

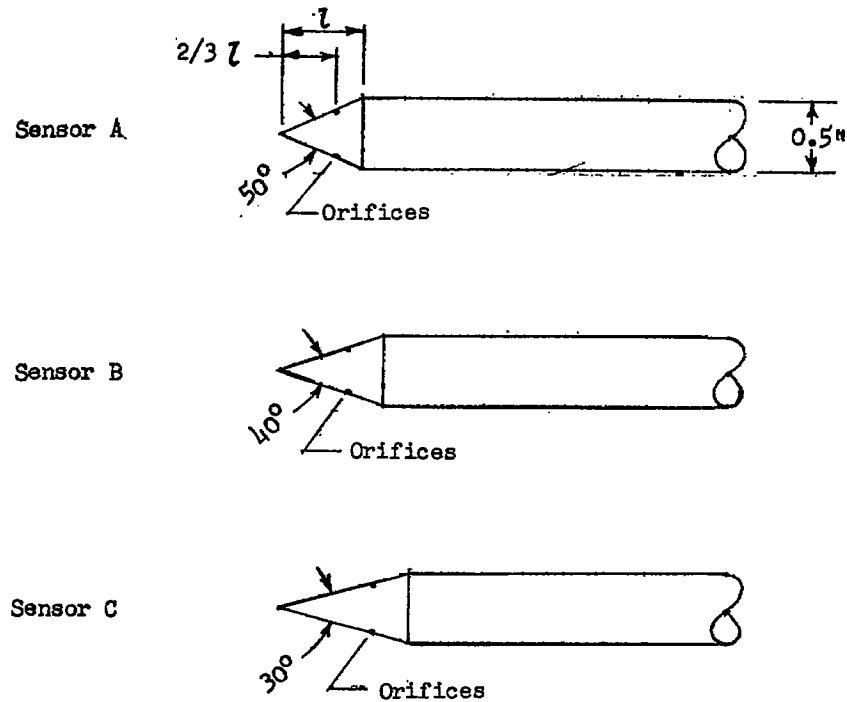


(a) Sensors.

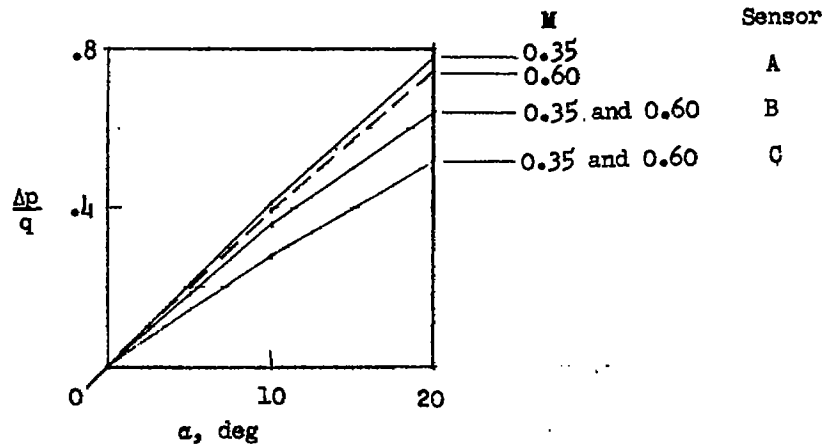


(b) Calibration.

Figure 4.- Variation of $\Delta p/q$ with α of two differential pressure sensors having hemispherical nose shapes (data from Cornell Aero. Lab., Inc.). $\beta = 0^\circ$.



(a) Sensors.

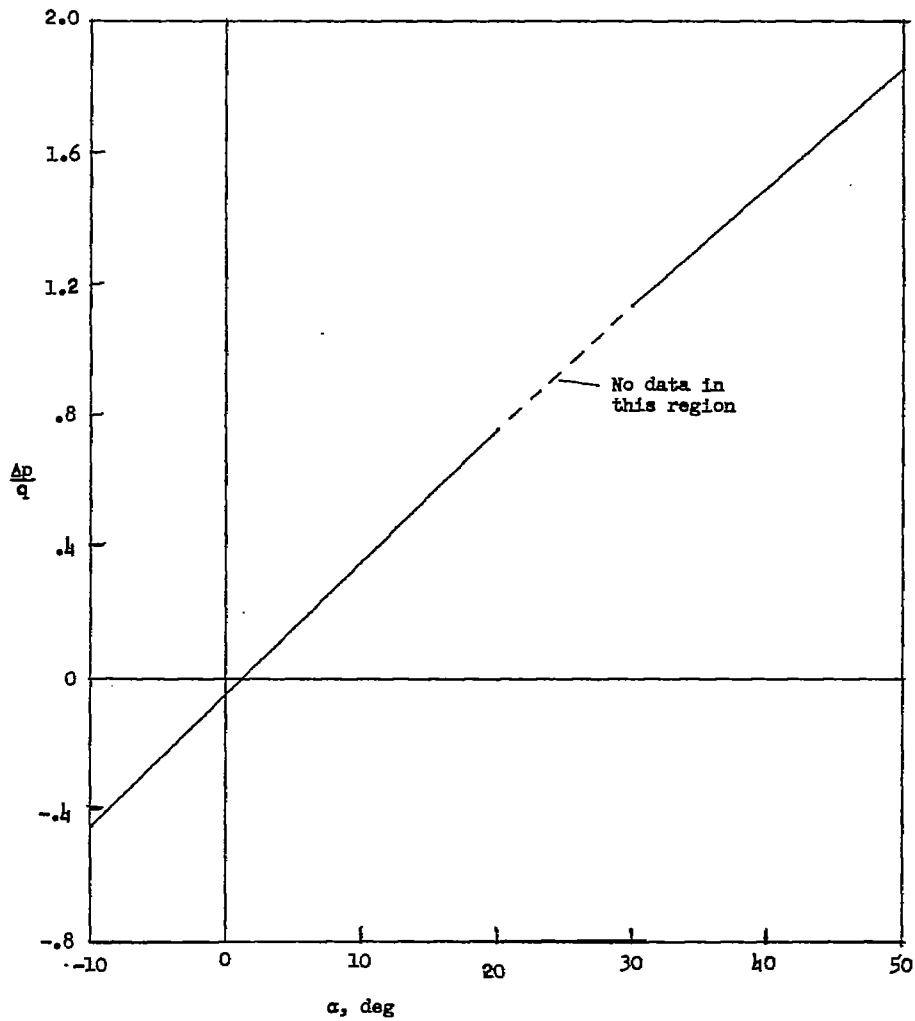


(b) Calibration.

Figure 5.- Variation of $\Delta p/q$ with α of three differential pressure sensors having conical nose shapes. Subsonic speeds (data from Cornell Aero. Lab., Inc.); $\beta = 0^\circ$.

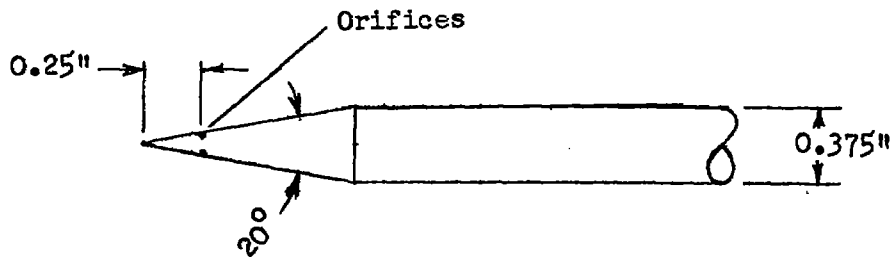


(a) Sensor.

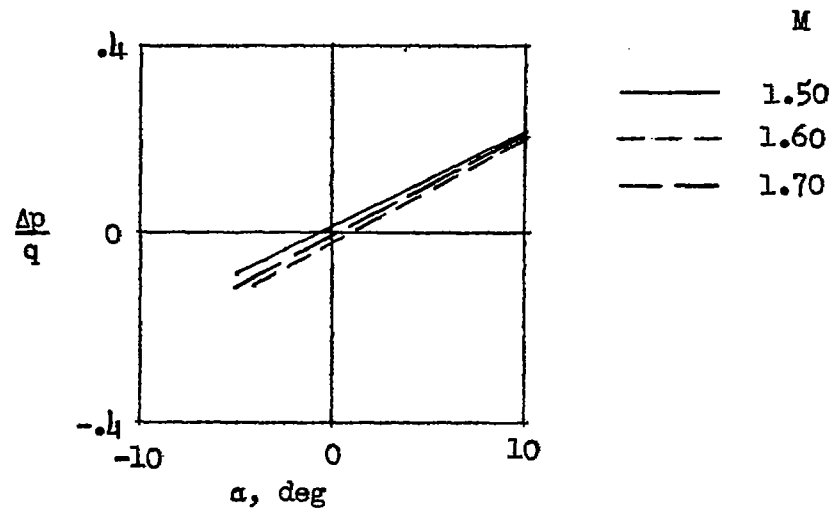


(b) Calibration.

Figure 6.- Variation of $\Delta p/q$ with α of a differential pressure tube having a conical nose shape. $M = 0.70$ to 1.10 (ref. 10); $\beta = 0^\circ$.

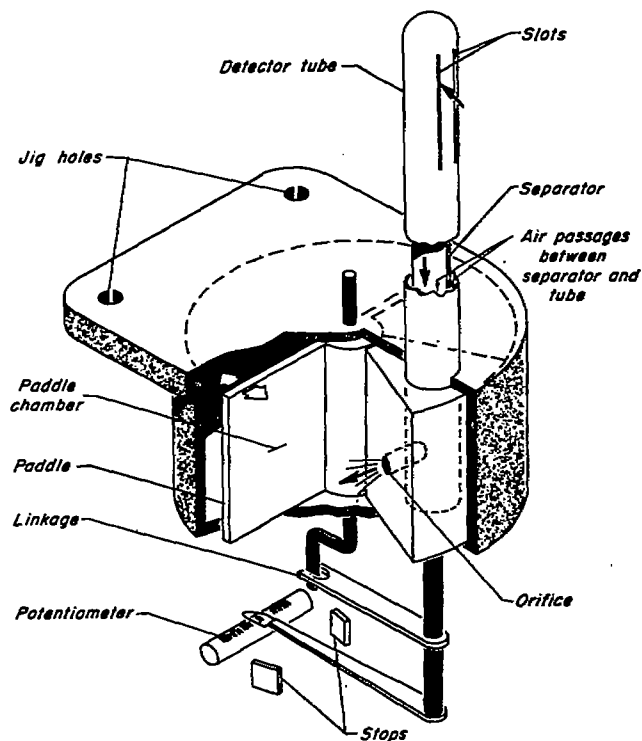


(a) Sensor.

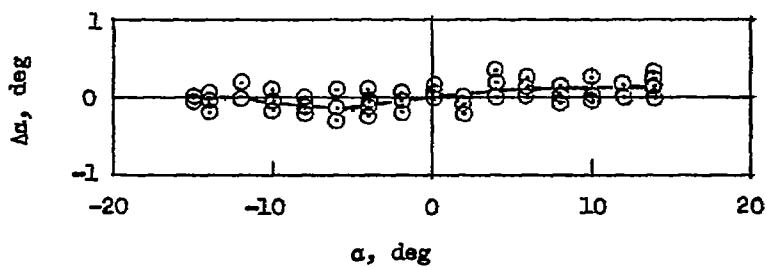


(b) Calibration.

Figure 7.- Variation of $\Delta p/q$ with α of a differential pressure tube having a conical nose shape. Supersonic speeds (ref. 11); $\beta = 0^\circ$.

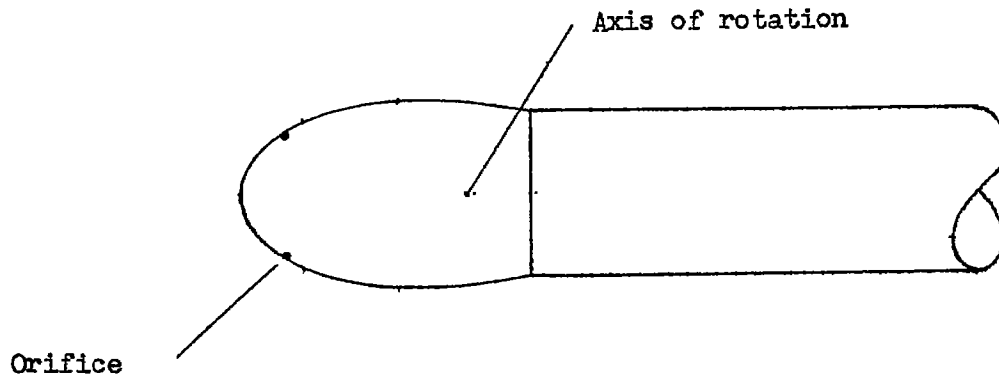


(a) Sensor.

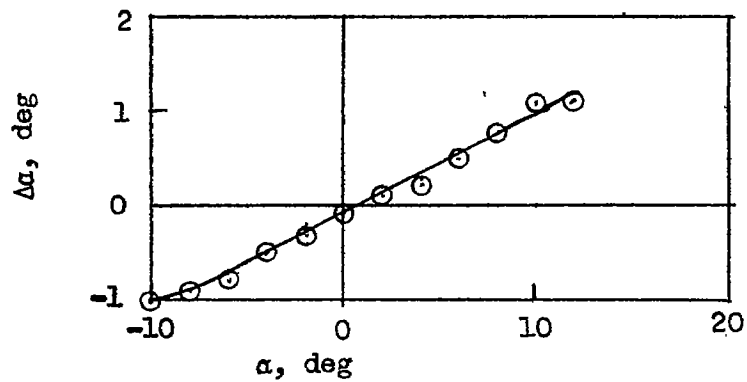


(b) Calibration.

Figure 8.- Calibration of null-seeking pressure-type angle-of-attack sensor. $M = 0.10$ (ref. 12); $\beta = 0^\circ$.

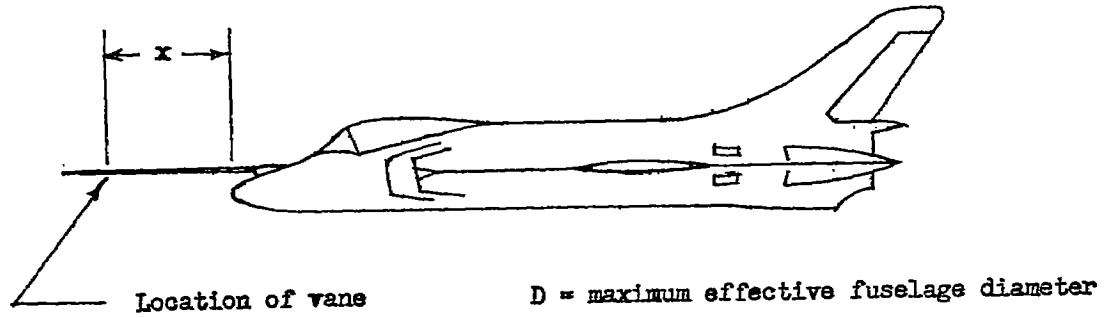


(a) Sensor.



(b) Calibration.

Figure 9.- Calibration of null-seeking pressure-type angle-of-attack sensor (ref. 8). $\beta = 0^\circ$.



(a) Sensor location on airplane.

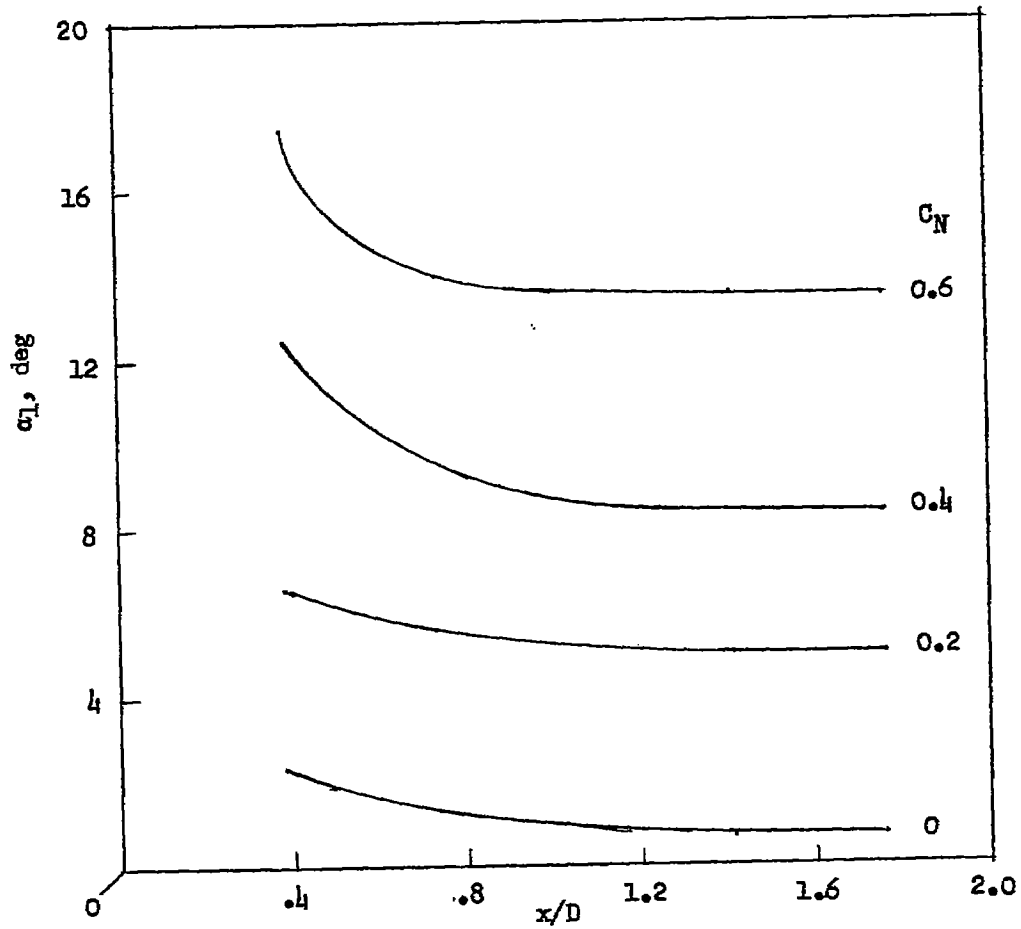
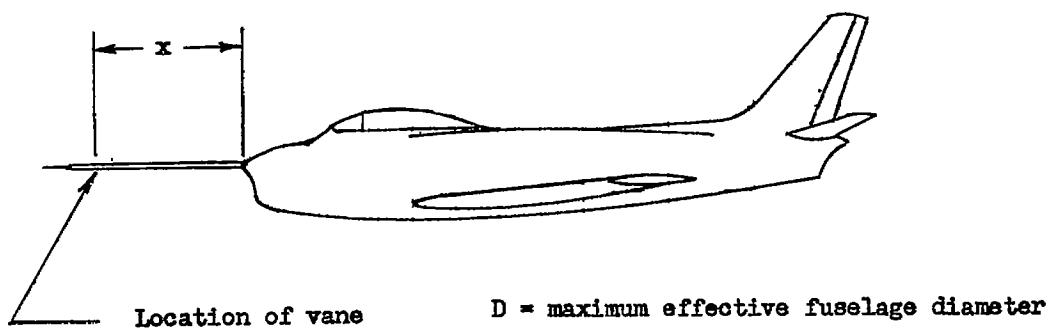
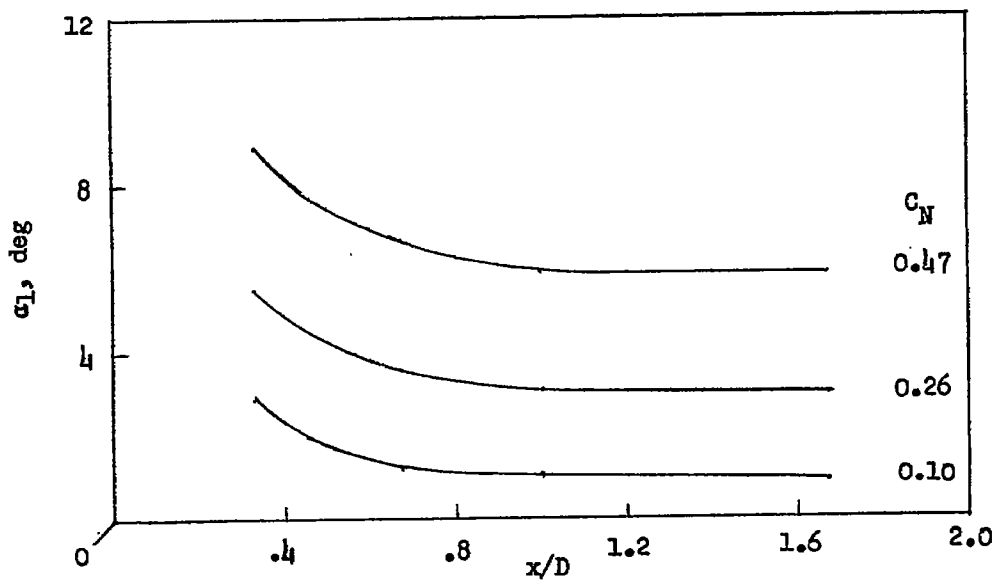
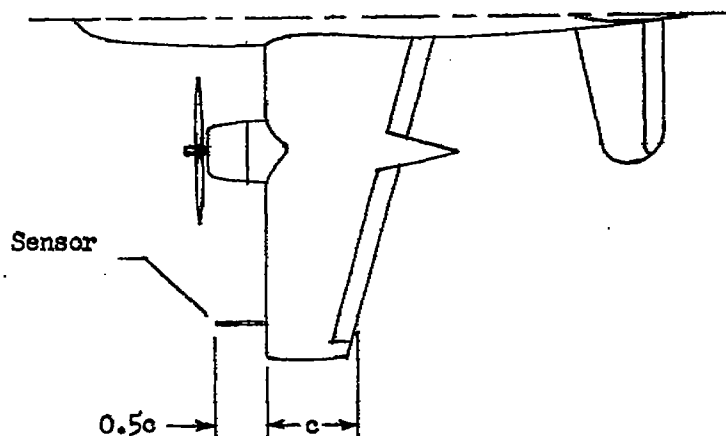
(b) Variation of α_1 with x/D .

Figure 10.- Variation of local angle of attack with distance ahead of a fuselage having an ogival nose with rounded tip (data from Ames Aero. Lab.). $M = 0.80$.

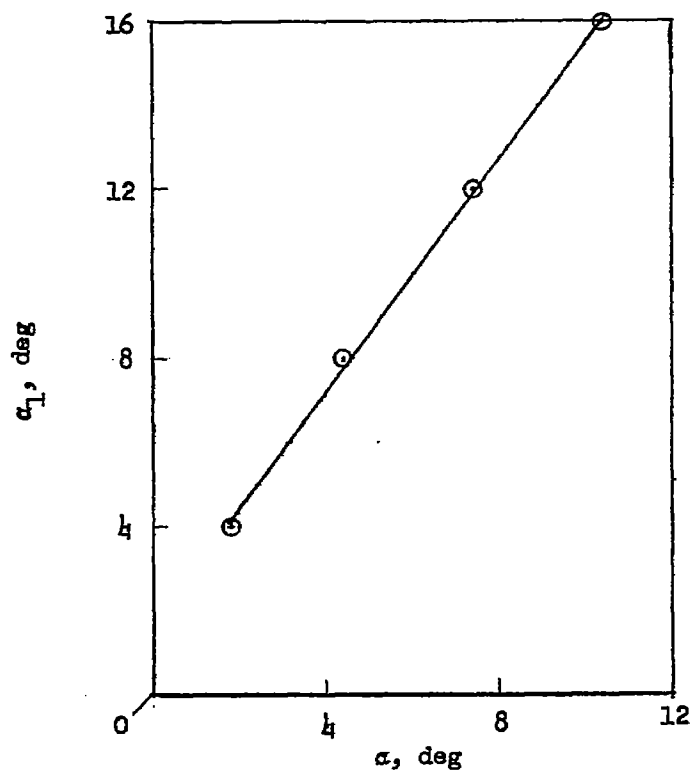


(a) Sensor location on airplane.

(b) Variation of α_1 with x/D .Figure 11.- Variation of local angle of attack with distance ahead of a fuselage having a nose inlet. $M = 0.81$ (ref. 13).

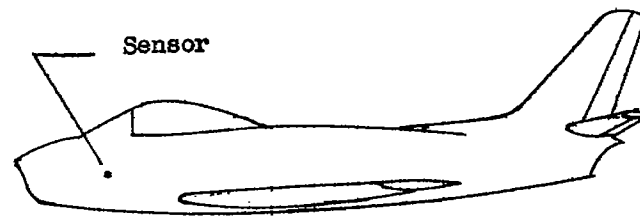


(a) Sensor location on airplane.

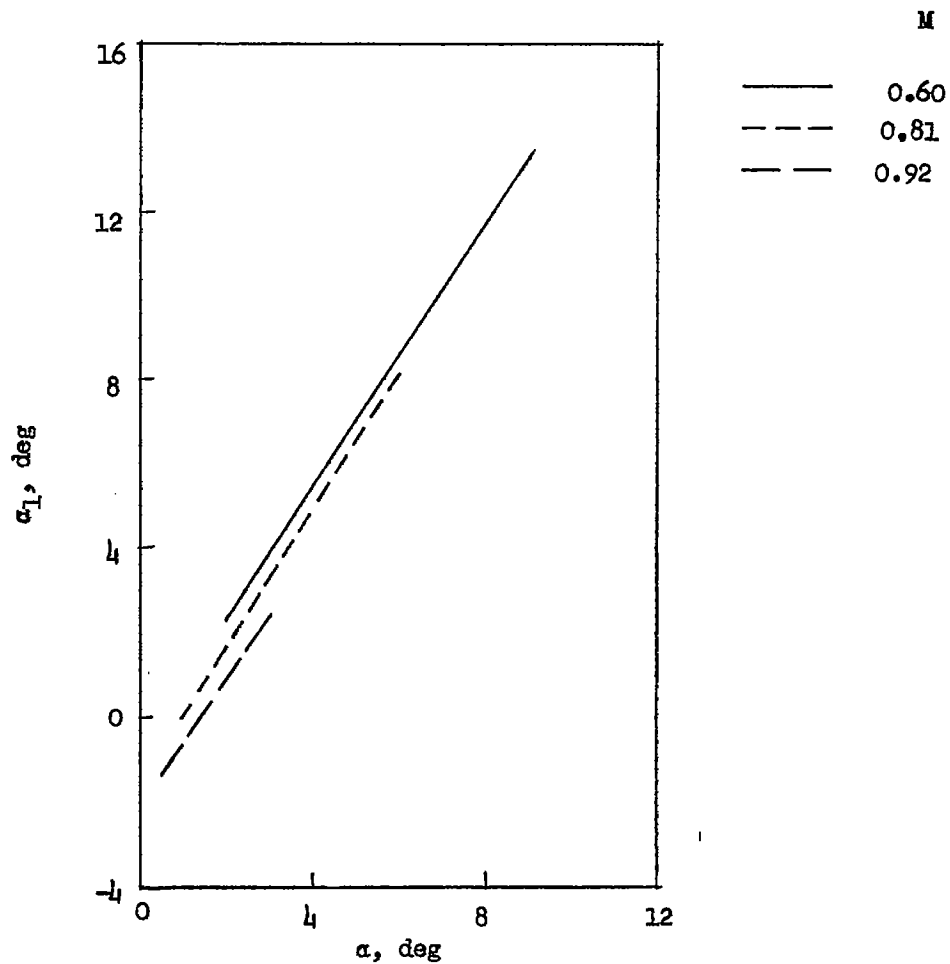


(b) Calibration.

Figure 12.- Flight calibration of an angle-of-attack sensor located 0.5 chord length ahead of the wing tip of an airplane. $M = 0.30$ (data from Cornell Aero. Lab., Inc.).



(a) Sensor location on airplane.



(b) Calibration.

Figure 13.- Flight calibration of null-seeking pressure-type angle-of-attack sensor (of the type shown in fig. 8) installed on the fuselage nose of an airplane (ref. 13).

	M	α , deg
————	0.70	3.8
-----	0.82	2.6
— — —	0.90 and 0.91	2.0

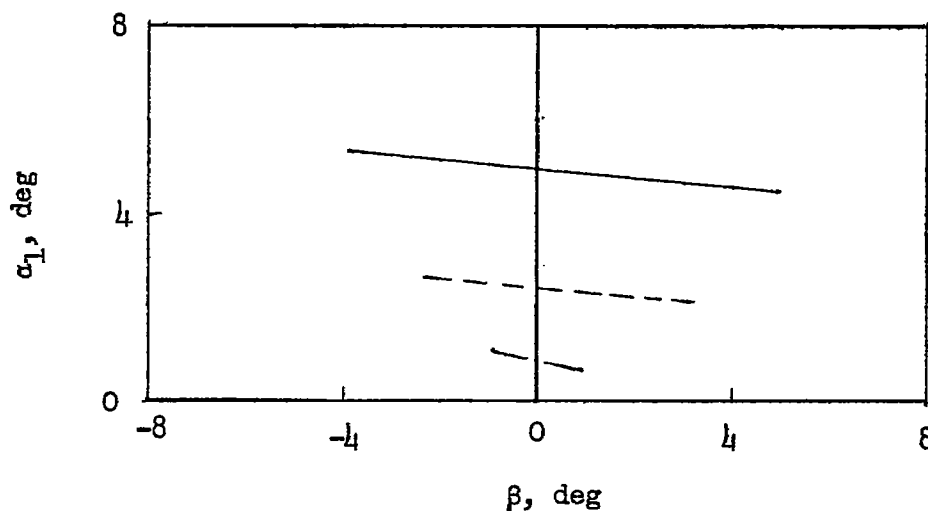


Figure 14.- Effect of sideslip on the angle of attack measured by null-seeking pressure-type sensor (of the type shown in fig. 8) installed on the fuselage nose of an airplane (ref. 13). Installation was the same as that shown in figure 13.